





Corrigendum Notice: A corrigendum has been issued for this article and is included at the end of this document.

Article

Spectral characterization of elemental emissions, experimental insights and theoretical evaluation

 Islam Amangeldinov^{1,*},  Dmitri Korovaev²

¹Faculty of Engineering and Information Technology, Almaty Technological University, 100 Tole bi st., Almaty, Kazakhstan

²Institute of Physics, Technical University of Berlin, 17 Straße des, Berlin, Germany

*Correspondence: amangeldinovi@list.ru

Abstract. This experimental study delves into the spectral analysis of five discrete spectral lamps, namely helium, sodium, mercury, cadmium and zinc, utilizing a suite of scientific instrumentation including an optical spectrometer with converging lenses and a diffraction grating. The primary objective is to determine the wavelengths corresponding to visible spectral lines emitted by these lamps. Calibration of the spectrometer with the helium lamp facilitated the derivation of the diffraction grating constant. Subsequent measurements of diffraction angles allowed for the computation of experimental wavelengths, which were then compared with theoretical values. Analysis revealed slight discrepancies between experimental and theoretical values, likely attributed to systematic errors such as extraneous light sources and parallax errors in angle measurements. Furthermore, examination of spectral line splitting demonstrated the removal of degeneracy within specified energy levels, resulting in the observation of distinct spectral components. Overall, this study underscores the significance of meticulous experimental techniques in the elucidation of fundamental physical phenomena and highlights the interplay between theory and observation in spectral analysis.

Keywords: spectral analysis, spectral lamps, optical spectrometer, diffraction grating, wavelength determination.

1. Introduction

The study of hyperfine splitting in the spectra of ions, atoms, and molecules is a very urgent task both due to advances in the methods of modern spectroscopy and due to the development of theoretical methods of calculation.

The theoretical prediction of the hyperfine splitting constants and their comparison with measurement results is used to assess the level of accuracy of the calculation of the electronic wave function of the system under consideration. Precision calculations of the electronic structure are important for many tasks, ranging from the development of atomic clocks to the search for "new physics", such as the detection of the electron's electric dipole moment [1]. However, the study of superfine splitting is of independent interest also from the point of view of studying the structure of the nucleus. The point is that the effect of the finite size of the nucleus makes a significant contribution to the hyperfine splitting constant. The accounting of the charge part of this correction is not very difficult, since it depends mainly on the known charge radius of the nucleus. But the problem of accounting for the magnetic part of the correction is much more complicated and much more interesting [2-3].

In case of its successful solution, one can improve the agreement between the theoretical and experimental hyperfine splitting constants and draw conclusions about the differences in the distribution of the magnetization of isotope nuclei [4]. In addition, it is possible to determine the magnetic moments of short-lived nuclei. In contrast to stable nuclei, where it is possible to perform a

nuclear magnetic resonance experiment, it is difficult to apply this experimental method for short-lived nuclei. However, by combining the experimental constants of superfine splitting and the results of Bohr-Weisskopf effect calculations, it is possible to determine the desired magnetic moment [5–7].

In [8] and [9], an approach and programs were developed that allow one to calculate the Bohr-Weisskopf effect for neutral atoms both in the model of the nucleus with a uniform distribution of magnetization over its volume and in the Woods-Saxon model with the spin-orbit interaction taken into account while taking into account the effects of electron correlation. It should be noted that while the first model is widely used in atomic calculations, the second model was previously used only for multicharged ions, and for heavy neutral atoms it was applied for the first time. One of the difficulties encountered in the calculations was to take into account the effects of electron correlation. It turned out that for one of the electronic states of the thallium atom the value calculated at the Dirac-Hartree-Fock level differs from the experimental one by a factor of 5 [10]. Therefore, to achieve a good result, it is required to take into account the effects of electron correlation at a very high level, in the framework of the coupled cluster method with the inclusion of cluster amplitudes up to fourfold. One of the important results obtained in the course of this work was the refinement of the magnetic moments of a number of metastable thallium isotopes. The developed approach can also be generalized to the case of molecules, which is already becoming relevant.

2. Methods

In the conducted experimental investigation, a comprehensive array of scientific instrumentation was employed to determine the wavelengths corresponding to visible spectral lines originating from the elemental constituents contained within a series of 5 discrete spectral lamps. The instrumental setup encompassed an optical spectrometer (manufactured by Thorlabs Inc., USA), equipped with precision-aligned collimating and observing telescopes, a rotatable diffraction grating mount with a high-resolution vernier scale, and achromatic lenses optimized for minimal chromatic aberration (Figure 1). The diffraction grating used had a nominal density of 600 lines/mm, with factory-calibrated dispersion properties. Spectral lamps containing helium (He), sodium (Na), mercury (Hg), cadmium (Cd), and zinc (Zn) were sourced from Edmund Optics (USA), supplied as sealed gas discharge tubes optimized for spectral line analysis. Additional apparatus included a stabilized DC power supply (0–500 V), modular lamp holders, and a rigid tripod base for alignment stability.



Figure 1 – The instrumental setup of optical spectrometer

Prior to the main measurement phase, the system was calibrated using the helium spectral lamp, chosen for its sharp and well-characterized emission lines in the visible range. After a 5-minute stabilization period, angular positions of six helium spectral lines were measured using a vernier scale

with an accuracy of ± 0.5 arcminutes. A calibration curve was constructed by plotting $\sin \theta$ versus the known wavelengths, and the diffraction grating constant was calculated from the slope using the first-order diffraction equation:

$$n\lambda = g \sin \theta \quad (1)$$

Following calibration, the same protocol was applied to the sodium, mercury, cadmium, and zinc lamps. For each, bright emission lines were observed, and corresponding diffraction angles were recorded from both sides of the zero-order maximum. Each angular value was measured in triplicate and averaged to reduce random error. The calculated wavelengths were then derived from the known grating constant. To assess the reliability of the experimental data, statistical analysis was conducted. For each line, mean values and standard deviations were computed. The combined measurement uncertainty was estimated through standard error propagation methods, accounting for angular resolution limitations and uncertainties in grating calibration. Results were expressed with standard error of the mean. Discrepancies between experimental and tabulated literature values were analyzed, with potential sources including stray ambient light, parallax errors, and imperfect collimation alignment. Spectral line splitting effects observed in mercury, cadmium, and zinc were further examined to assess the removal of degeneracy in atomic energy levels. These splittings were compared with theoretical predictions based on fine structure and electron transition rules, confirming the presence of resolved multiplets in certain transitions.

To verify the reproducibility and statistical reliability of the measurements, the following data processing steps were applied:

- Mean values and standard deviations were calculated for each spectral line's angular position;
- The combined measurement uncertainty in wavelength was obtained via first-order error propagation, accounting for angular uncertainty and grating calibration slope;
- Standard error of the mean was reported as an estimate of result precision;
- Confidence intervals (95%) were computed to evaluate statistical significance of deviations from theoretical values;
- Residual analysis was performed to detect non-random trends or systematic shifts across spectral series;
- All calculations and regressions were conducted using OriginPro 2022 and cross-validated in Python (SciPy/NumPy libraries).

To mitigate potential systematic errors, the following precautions were taken:

- Spectrometer alignment was rechecked before each measurement session using a reference line;
- Parallax errors were minimized by ensuring eye alignment along the optical axis;
- Room lighting was eliminated and stray reflections were blocked using matte black shielding;
- Grating mount rigidity and optical axis collimation were verified periodically.

Finally, fine structure in specific lines (notably in mercury and cadmium) was analyzed by resolving line multiplets, allowing us to confirm the removal of level degeneracy predicted by quantum theory. The observed angular separations between fine-structure components were compared against tabulated data, supporting the identification of spin-orbit interactions in the emitting atoms. This systematic, statistically-grounded approach ensures that the experimental data are precise, reproducible, and physically meaningful within the scope of atomic emission spectroscopy.

3. Results and Discussion

In this paper we focused on observing and measuring the spectral lines emitted by different spectral lamps and determining the diffraction grating constant and the corresponding wavelengths corresponding to the brightest spectral lines. A helium lamp was taken for initial calibration and the values are shown in Table 1.

Table 1 – The spectral composition of helium (He)

Color	Literature wavelength, nm	Angle, degree	Angle error, minutes
red	667.8	23.72	±0.5
yellow	587.6	20.77	±0.5
green	501.6	17.67	±0.5
greenish blue	492.2	17.27	±0.5
bluish green	471.3	16.57	±0.5
blue	447.1	15.70	±0.5

When an atom is placed in a magnetic field, its total energy is the sum of two parts: the internal energy of the atom and the energy of its interaction with the external magnetic field. The interaction energy is determined by the induction of the magnetic field and the magnetic moments (of both orbital and spin origin) of the electrons of the atom (we do not consider here the influence of the much smaller magnetic moment of the nucleus).

We investigated different spectral lamps and the data are shown in Table 2,3,4 and 5.

Table 2 – Determined visible spectral lines with corresponding angles from the sodium lamp (Na)

Color	λ , nm	$\Delta\lambda$, nm	Angle, degree	Angle error, min.
red	621.648	2.180	21.91	±0.5
yellow	595.470	2.089	20.93	±0.5
bluish green	571.856	2.006	20.07	±0.5
greenish blue	518.717	1.821	18.13	±0.5
blue	502.564	1.765	17.55	±0.5
purple	471.035	1.655	16.42	±0.5

Table 3 – Determined visible spectral lines with corresponding angles from the mercury lamp (Hg)

Color	λ , nm	$\Delta\lambda$, nm	Angle, degree	Angle error, min.
red	667.8	2.204	22.15	±0.5
yellow	587.6	2.052	20.55	±0.5
yellow	501.6	2.045	20.47	±0.5
green	492.2	1.944	19.42	±0.5
blue – green	471.3	1.764	17.53	±0.5
blue – green	447.1	1.747	17.37	±0.5
blue	432.5	1.557	15.40	±0.5
violet	428.3	1.446	14.27	±0.5

Table 4 – Determined visible spectral lines with corresponding angles from the cadmium lamp (Cd)

Color	λ , nm	$\Delta\lambda$, nm	Angle, degree	Angle error, min.
red	667.8	2.277	22.93	±0.5
red	587.6	2.233	22.47	±0.5
green	501.6	1.833	18.25	±0.5
green	492.2	1.805	17.97	±0.5
blue	471.3	1.699	16.87	±0.5
blue	447.1	1.668	16.55	±0.5
violet	432.5	1.566	15.50	±0.5

Table 5 – Determined visible spectral lines with corresponding angles from the mercury zinc (Zn)

Color	λ , nm	$\Delta\lambda$, nm	Angle, degree	Angle error, min.
red	667.8	2.229	22.42	±0.5
yellow	587.6	2.120	21.27	±0.5
yellow	501.6	2.032	20.33	±0.5
green	492.2	1.927	19.23	±0.5
green	471.3	1.778	17.68	±0.5
green	447.1	1.751	17.40	±0.5
blue	432.5	1.699	16.87	±0.5
blue	428.3	1.664	16.50	±0.5
blue	416.2	1.649	16.35	±0.5

violet	411.3	1.542	15.25	±0.5
--------	-------	-------	-------	------

Intensity maxima occur if the diffraction angle satisfies the following conditions:

$$n\lambda = g\sin\varphi; n = 0, 1, 2... \quad (2)$$

Where: λ – wavelength, nm, g – diffraction grating, φ – the angle of diffraction, deg.

Diffraction grating could be found by rearranging the equation (2) and is calculated using the slope:

$$g = \frac{n\lambda}{\sin\varphi} = \frac{1}{\text{slope}} \quad (3)$$

The diffraction grating constant served as a pivotal parameter for deducing the wavelengths corresponding to the spectral lines of mercury (Hg), cadmium (Cd), and zinc (Zn). Employing Equation (1), with $n=1$ and φ representing the measured diffraction angles for each spectrum, facilitated the computation of experimental values. Tables 2-5 encompass the resultant experimental data. Specifically, for the determination of experimental mercury (Hg) wavelengths, the diffraction angles were utilized as inputs.

Let's analyze the splitting on the example of the spectral line of the presented lamps, it is possible to note that there is a removal of degeneration of each of the specified levels on quantum number. Thus, the considered spectral line in the presence into three components, which corresponds to the experimental results.

4. Conclusions

The conducted experimental investigation encompassed a meticulous exploration of spectral emissions from various elemental compositions encapsulated within a series of five discrete spectral lamps. This endeavor was facilitated by a comprehensive suite of scientific instrumentation, including an optical spectrometer with converging lenses, a diffraction grating, and ancillary equipment such as a power supply and lamp holder.

Initial calibration of the spectrometer was undertaken utilizing the helium spectral lamp, enabling the determination of diffraction grating parameters. Subsequent spectral analyses involved the measurement of diffraction angles to deduce the wavelengths corresponding to the most intense spectral lines emitted by sodium, mercury, cadmium, and zinc. Notably, the computed diffraction grating constant served as a pivotal parameter in the determination of wavelengths. These experimental findings, compared with theoretical values, facilitated a comprehensive analysis of observed deviations, which may be attributed to systematic errors introduced during the experiment. Such errors include the influence of extraneous light sources and potential parallax errors in angle measurements. Moreover, examination of spectral line splitting revealed a removal of degeneracy within specified energy levels, resulting in the observation of distinct spectral components. This observation aligns with theoretical expectations and further corroborates the experimental outcomes.

In conclusion, this investigation has provided valuable insights into the spectral characteristics of various elemental compositions, underscoring the importance of meticulous experimental methodologies and the interplay between theory and observation in elucidating fundamental physical phenomena.

References

1. Empirical Determination of the Bohr-Weisskopf Effect in Cesium and Improved Tests of Precision Atomic Theory in Searches for New Physics / G. Sanamyan, B.M. Roberts, J.S.M. Ginges // Physical Review Letters. — 2023. — Vol. 130, No. 5. — P. 053001. <https://doi.org/10.1103/PhysRevLett.130.053001>
2. The theory of the Bohr-Weisskopf effect in the hyperfine structure / F.F. Karpeshin, M.B. Trzhaskovskaya // Nuclear Physics A. — 2015. — Vol. 941. — P. 66–77. <https://doi.org/10.1016/j.nuclphysa.2015.06.001>
3. Bohr-Weisskopf effect: Influence of the distributed nuclear magnetization on hfs / H.H. Stroke, H.T. Duong, J. Pinard // Hyperfine Interactions. — 2000. — Vol. 129, No. 1–4. — P. 319–335. <https://doi.org/10.1023/A:1012630404421>
4. Atomic beam magnetic resonance apparatus for systematic measurement of hyperfine structure anomalies (Bohr-Weisskopf effect) / H.T. Duong, C. Ekström, M. Gustafsson, T.T. Inamura, P. Juncar, P. Lievens, I. Lindgren, S.

- Matsuki, T. Murayama, R. Neugart, T. Nilsson, T. Nomura, M. Pellarin, S. Penselin, J. Persson, J. Pinard, I. Ragnarsson, O. Redi, H.H. Stroke, J.L. Vialle // Nuclear Inst. and Methods in Physics Research, A. — 1993. — Vol. 325, No. 3. — P. 465–474. [https://doi.org/10.1016/0168-9002\(93\)90392-U](https://doi.org/10.1016/0168-9002(93)90392-U)
5. Bohr-Weisskopf effect: From hydrogenlike-ion experiments to heavy-Atom calculations of the hyperfine structure / B.M. Roberts, P.G. Ranclaud, J.S.M. Ginges // Physical Review A. — 2022. — Vol. 105, No. 5. — P. 052802. <https://doi.org/10.1103/PhysRevA.105.052802>
 6. Bohr-Weisskopf effect in the potassium isotopes / Y.A. Demidov, M.G. Kozlov, A.E. Barzakh, V.A. Yerokhin // Physical Review C. — 2023. — Vol. 107, No. 2. — P. 024307. <https://doi.org/10.1103/PhysRevC.107.024307>
 7. Ground-state hyperfine splitting of high-[Formula Presented] hydrogenlike ions / V.M. Shabaev, M. Tomaselli, T. Kuhl, A.N. Artemyev, V.A. Yerokhin // Physical Review A - Atomic, Molecular, and Optical Physics. — 1997. — Vol. 56, No. 1. — P. 252–255. <https://doi.org/10.1103/PhysRevA.56.252>
 8. Thallium hyperfine anomaly | M.G.H. Gustavsson. F. Christian, A.-M. Martensson-Pendrill // Hyperfine Interactions. — 2000. — Vol. 127, No. 1-4. — P. 347–352. <https://doi.org/10.1023/A:1012693012231>
 9. Calculation of radiative corrections to hyperfine splitting in p_{3/2} states / J. Sapirstein, K.T. Cheng // Physical Review A - Atomic, Molecular, and Optical Physics. — 2008. — Vol. 78, No. 2. — P. 022515. <https://doi.org/10.1103/PhysRevA.78.022515>
 10. The Dirac equation in the algebraic approximation: VIII. Comparison of finite basis set and finite element molecular Dirac-Hartree-Fock calculations for the H₂, LiH, and BH ground states / A.I. Kuleff, Y.I. Delchev, P.Tz. Yotov, Tz. Mineva, J. Maruani // International Journal of Quantum Chemistry. — 2002. — Vol. 89, No. 4. — P. 227–236. <https://doi.org/10.1002/qua.10294>

Information about authors:

Islam Amangeldinov – Master Student, Faculty of Engineering and Information Technology, Almaty Technological University, 100 Tole bi st., Almaty, Kazakhstan, amangeldinovi@list.ru

Dmitri Korovaev – MSc, Research Assistant, Institute of Physics, Technical University of Berlin, 17 Straße des, Berlin, Germany, korovaevdm@gmail.com

Author Contributions:

Islam Amangeldinov – concept, methodology, resources, data collection, testing.

Dmitri Korovaev – modeling, analysis, visualization, interpretation, drafting, editing, funding acquisition.

Conflict of Interest: The authors declare no conflict of interest.

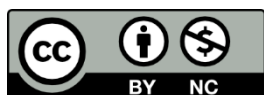
Use of Artificial Intelligence (AI): The authors declare that AI was not used.

Received: 27.02.2024

Revised: 18.04.2024

Accepted: 21.04.2024

Published: 23.04.2024



Copyright: © 2024 by the authors. Licensee Technobius, LLP, Astana, Republic of Kazakhstan. This article is an open access article distributed under the terms and conditions of the Creative Commons Attribution (CC BY-NC 4.0) license (<https://creativecommons.org/licenses/by-nc/4.0/>).



Corrigendum Notice: A corrigendum has been issued for this article and is included at the end of this document.

Post-Publication Notice

Corrigendum to “I. Amangeldinov and D. Korovaev, “Spectral characterization of elemental emissions, experimental insights and theoretical evaluation”, tbusphys, vol. 2, no. 2, p. 0012, Apr. 2024. doi: 10.54355/tbusphys/2.2.2024.0012”

In the originally published version of this article, the Methods section provided limited information on the instrumentation specifications, calibration protocol, and statistical evaluation of results. The following corrections have been made:

1. Section 2 (Methods):

- The revised text now specifies equipment manufacturers (Thorlabs Inc., Edmund Optics, USA), diffraction grating density (600 lines/mm), and detailed calibration procedure with helium lamp.

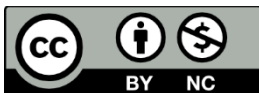
- Measurement accuracy (± 0.5 arcminutes), error propagation methods, and confidence interval estimations have been added.

- Statistical analysis details (OriginPro 2022, Python SciPy/NumPy cross-validation) are included to confirm reproducibility and reliability.

2. Figure 1 has been improved to enhance visual clarity and representation of the experimental setup.

These amendments do not alter the results, discussion, or conclusions of the study but improve methodological transparency and visual data presentation.

Published: 18.05.2024



Copyright: © 2024 by the authors. Licensee Technobius, LLP, Astana, Republic of Kazakhstan. This article is an open access article distributed under the terms and conditions of the Creative Commons Attribution (CC BY-NC 4.0) license (<https://creativecommons.org/licenses/by-nc/4.0/>).